Springer

KSME

Journal of Mechanical Science and Technology 31 (2) (2017) 615~623
www.springerlink.com/content/1738-494x(Print)/1976-3824(Online)
DOI 10.1007/s12206-017-0114-4

Prediction of the hardness profile of an AISI 4340 steel cylinder heat-treated by laser - 3D and artificial neural networks modelling and experimental validation †

Mahdi Hadhri, Abderazzak El Ouafi* and Noureddine Barka

Mathematics, Computer Science and Engineering Department, University of Quebec at Rimouski, Canada

(Manuscript Received February 11, 2016; Revised September 6, 2016; Accepted September 28, 2016)

Abstract

This paper presents a comprehensive approach developed to design an effective prediction model for hardness profile in laser surface transformation hardening process. Based on finite element method and Artificial neural networks, the proposed approach is built progressively by (i) examining the laser hardening parameters and conditions known to have an influence on the hardened surface attributes through a structured experimental investigation, (ii) investigating the laser hardening parameters effects on the hardness profile through extensive 3D modeling and simulation efforts and (ii) integrating the hardening process parameters via neural network model for hardness profile prediction. The experimental validation conducted on AISI4340 steel using a commercial 3 kW Nd:Yag laser, confirm the feasibility and efficiency of the proposed approach leading to an accurate and reliable hardness profile prediction model. With a maximum relative error of about 10 % under various practical conditions, the predictive model can be considered as effective especially in the case of a relatively complex system such as laser surface transformation hardening process.

Keywords: Superficial heat treatment; Laser surface transformation hardening; AISI 4340 steel; Hardness profile prediction; Finite element method; Artificial neural network; Design of experiments

1. Introduction

Superficial heat treatment is an essential and complex process in manufacturing technology. The major objective of superficial hardening is to optimize the performance of operating mechanical components by modifying their physical, chemical and metallurgical properties.

The most common methods of heat treatment include flame, induction, carburizing and nitriding. The disadvantages of these methods, such as the complexity of equipment for some and problems with parameter control for others, lead to the use of high power lasers as a new heat treatment process. The first heat treatment of metals by laser took place in the early 1960s. In the following years, much research was performed on the superficial hardening of steel which allowed the use of the laser. At the outset, researchers were interested in understanding the influence of certain parameters (such as scanning speed, laser power, wavelength, beam diameter, etc.) on the temperature, hardness and depth of the treatment on flat geometries. Finite element models were created based on the Rosenthal equation of a moving heat source [1].

In another stage, some researchers became interested in the modeling of the temperature distribution on cylindrical piece during treatment, in order to predict the microstructure, hardening depth, hardness, and residual stresses.

Patwa and Shin achieved a 3D finite element model [2]. The model combines a transient digital three-dimensional solution (based on the modeling of Rozzi et al. [3, 4]) for a rotary cylinder undergoing laser heating by translation of the beam with a kinetic model. In order to evaluate the simulation results, an experiment was performed. Both researches reach a depth of 0.54 mm with a hardness of 63 HRC on an AISI 5150 steel specimen with a laser (diode) power of 500 W and a rotational speed of 6 rpm [2]. Skvarenina et al. also predicted experimentally and successfully reached a 2.5 mm hardening depth with a uniform hardness of 57 HRC on an AISI 1536 steel cylinder 60 mm in diameter, using a scanning speed of 2.9 mm/s, a laser (diode) power of 1220 W and a rotational speed of 1 rpm [5]. Another thermal transient 3D model was developed by Orazi et al. [6]. The model is based on the geometry of the ring spot and was validated by experimental tests. The advantage of the Leonardo model over other models is that it achieves very high speeds. For a rotational speed of 1140 rpm, a power of 1 kW, a scanning speed of 30 mm/min and a 30 mm diameter test piece of AISI 1040 steel, it finds a hardness of 690 HV. In general, a second laser pass generates a tempering of the material that is characterized by a drop in

*Corresponding author. Tel.: +1 418 723 1986, Fax.: +1 418 724 1879
E-mail address: Abderrazak_ElOuafi@uqar.ca
† Recommended by Associate Editor Sang-Hee Yoon

micro hardness. In the same context, the low processing speed creates a superposition of treatment which pro-duce a non-homogeneous micro hardness.

The prediction of hardness by the finite element method has many advantages, namely minimizing costs and the experimentation time, but it remains a complex and specific tool depending on the case. In an industrial framework the objective is to develop rapid modeling that allows the implementation of a real time control strategy. The regulation and selection of optimal parameters is a challenge that must be addressed in a minimal amount of time. According to the literature, the most widely used methods of hardness predictions using laser heat treatment are linear multi-regression and artificial neural networks (ANN). Barka and El Ouafi found a mathematical model for the prediction of hardened depth based on the multi-regression method from a host of experimental tests on a 10 mm diameter cylinder. Using the Taguchi method, l9 experiments were planned with three factors at three levels. The various factors in the experiments are the scanning speed, the rotational speed and the laser power. With a power of 1700 W, a scanning speed of 4 mm/s and a rotary speed of 4000 rpm, a hardened depth of 1.9 mm was found [7]. A comparison between the two methods of hardness prediction on plates is performed by Maamri et al. An experimental study was done with 16 training experiments and 9 validation experiments. The factors that are considered in this study are laser power, scanning speed, hardness, initial hardness and surface state. In this study, it is confirmed using validation tests that the neural network method leads to the most useful prediction [8].

The main objective of this work is first to design a thermal model based on the finite element method coupled with a hardness prediction algorithm relying on the metallurgical transformation kinetics. The second objective is to carry out a host of laser heating tests to validate the digital model. Finally, using the 3D model and artificial neural networks, we develop a predictive model of the hardness profile based on various operating parameters.

2. Finite element modelling

In this study, the laser was modeled as a source of circular Gaussian heat moving along the shaft. As illustrated in Fig. 1, the shaft is mounted on test stand allowing a relatively high rotational speed (Fig. 1). In general, non-linear mathematical models of heat transfer by conduction in a homogeneous and isotropic medium take the following form:

$$\rho.C_p.\frac{dT}{dt}+\rho.C_p.u.\nabla T+\nabla(-k.\nabla T)=Q(x,y,z). \tag{1}$$

$Q(x,y,z)$ [W/m^3], which is the volume density of the laser applied to the material, is given by:

$$Q(x,y,z)=I(\mathrm{x,y}).(1-R_c).A_c.\exp(-A_c.z) \tag{2}$$

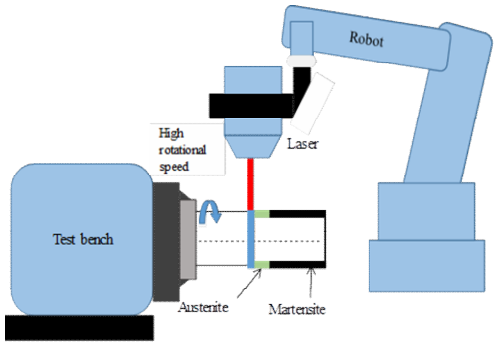

Fig. 1. Configuration of the laser hardening setup for cylindrical part.

where $I(x,y)$ [W/m^2], which is the intensity of the laser, and is given by:

$$I(x,y)=\frac{Q_0}{S}.f(x,y) \tag{3}$$

here Q_0 is the power of laser and S is the surface of the beam in contact with the material and $f(x, y)$ is the Gaussian distribution of the beam, given by:

$$f(x,y)=e^{-\left(\frac{(x-(x_0-V.t))^2}{2.w^2}+\frac{(y-y_0)^2}{2.w^2}\right)}. \tag{4}$$

x_0 and y_0 represent the beam center coordinates at $t = 0$. The effect of rotation of the piece is modeled by a transmission term in the heat transfer equation (Eq. (1)), so that it is not necessary to rotate the geometry explicitly. The boundary conditions were chosen as follows: The initial temperature of the system is supposed to be $T_0 = 293$ K; convection losses are taken into account given by Eq. (5) and radiation losses are considered negligible as compared to the incident radiation.

$$q_{conv}=(T-T_0)\int_{S_a} h\,dS_a \tag{5}$$

where h [$W/(m^2 \bullet K)$], which is the heat transfer coefficient and S_a is the area of the cylinder. Take into consideration the boundary conditions, the Eq. (1) becomes:

$$\rho.C_p.\frac{dT}{dt}+\rho.C_p.u.\nabla T+\nabla(-k.\nabla T)=Q(x,y,z)-q_{conv}. \tag{6}$$

For the mesh, the tetrahedral shape was chosen and a convergence study of the mesh size was carried out in order to choose the optimal size (Fig. 2).

3. Metallurgical modelling

The metallurgical transformation process for the heat treatment of steel occur over three major steps: The pearlite transformation to austenite (pearlite dissolution), the homogenization of the carbon in austenite, and the austenite transforma-

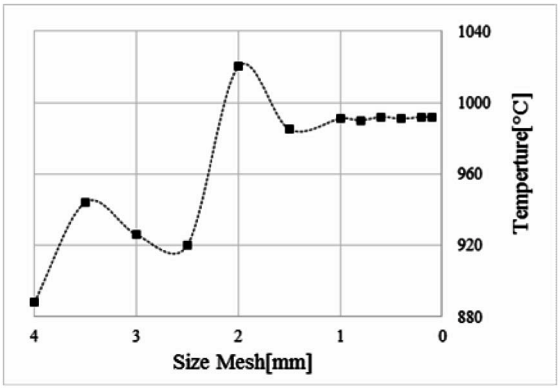

Fig. 2. Effect of mesh size on achieved temperatures.

tion to martensitic [9]. By heating the material up to the temperature of eutectoid Ac_1, colonies of pearlite in the microstructure are transformed into austenite. The distance between the pearlite plates, which allow colonies pearlite to be completely transformed into austenite, is given by the following equations [9].

$$I_p^2 = 2.D_0.c_d.\tau_h.e^{(-\frac{Q_a}{R_g.T_p})} \tag{7}$$

where D_0 is the diffusion constant, Q_a is the activation energy, R the gas constant, T_p is the peak temperature, and c_d and τ_h are constants given by Eqs. (8) and (9).

$$c_d = 3.\sqrt{\frac{R_g.T_p}{Q_a}} \tag{8}$$

$$\tau_h = \frac{(1-R_c).P}{2.\pi.K.eV.(T_p - T_0)}. \tag{9}$$

Here K the thermal conductivity, V is the scanning speed, T_0 is the initial temperature and R_c is the reflection coefficient. The homogenization mechanism is simple: Around a ferrite grain and a cementite grain, an austenite germ can be created. This germ is formed by eutectoid transformation with a chemical composition of 0.8 % C.

As the temperature rises it undergoes a systematic change in its composition. Rapid cooling of the austenite, which is formed only within a thin layer during laser hardening due to the self-sealing of the material when the laser beam is moved away, makes it difficult for carbon to diffuse outside its lattice. When the carbon is trapped in the network and cooled, the face-centered cubic crystal structure of austenite is transformed into a hybrid quadratic structure, called martensite [5]. The martensitic volume fraction, f, which is formed on a period T, is given by Eq. (10) [9].

$$f = f_m - (f_m - f_i)e^{-\left[\frac{12.f_i^{2/3}}{g_s.\sqrt{\pi}}\ln(\frac{C_e}{2.C_c}).\frac{l_p^2}{\sqrt{2}}\right]} \tag{10}$$

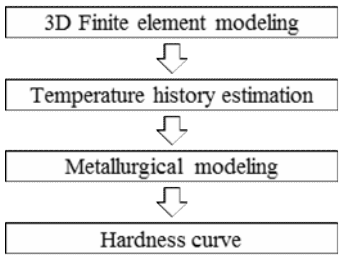

Fig. 3. Hardness curve estimation approach.

where $fi = C / 0.8$ is the initial volume fraction of pearlite and f_m is the volume fraction of martensite, given by the following relationship:

$$\begin{cases} 0 & \text{if } T_p < A_{c1} \\ f_i + (1-f_i)\dfrac{T_p - A_{c1}}{A_{c3} - A_{c1}} & \text{if } A_{c1} \le T_p \le A_{c3} \\ 1 & \text{if } T_p > A_{c1} \end{cases}. \tag{11}$$

The hardness of the material is calculated as follows:

$$H = f.H_m + (1-f).H_{f+p} \tag{12}$$

were H_m and H_{f+p} are calculated following Maynier's equations and taking into account the initial chemical composition [10, 11].

As explained in Fig. 3, the metallurgical equations are expressed in Matlab software. From the history of temperature matrix generated by the simulation, the algorithm is able to predict the hardness profile.

4. Simulation results

This study investigates the machine sensitivity parameters of laser heat treatment of an AISI 4340 steel shaft. The AISI 4340 steel is very common in the aerospace and automotive industries in the manufacture of propeller shafts, connecting rods, gear shafts and other parts, and automobiles due to its high tensile strength. The chemical composition and the material properties of the 4340 steel are presented in Tables 1 and 2. The laser heat treatment of a 10 mm diameter cylinder with a power of 1550 W, a scanning speed of 5 mm/s, and a rotary speed of 4000 rpm was simulated with the finite element model presented in the preceding section. Fig. 1 shows the profile where the temperature is greater than the austenitizing temperature and Fig. 2 shows that the heat flux propagation along the cylinder.

The interesting conclusion drawn from Figs. 4 and 5 is that the temperature does not increases abruptly at a given point, as in the case of the treatment of the plates, but rather gradually increases as the beam gets closer to the point. This is due to the rotation effect.

As demonstrated in Fig. 6, an increase in the power causes intensification in the maximum temperature reached. The

Table 1. Chemical composition of 4340 steel.

Elements	Content (wt %)
C	0.38 - 0.43
Cr	0.70 - 0.90
Mn	0.60 - 0.80
Mo	0.20 - 0.30
Ni	1.65 - 2.00
P	0.035
Si	0.15 - 0.35
S	0.004
Fe	95.195 - 96.33

Table 2. Material properties.

Property	Symbol	Unit	Value
Reflexion coefficient	Rc		0.6
Steel absorptivity	Ac	m-1	800
Eutectoid temperature	Ac1	K	996
Austenitization temperature	Ac3	K	1063,15
Austenite grain size (assumed)	g	µm	
Activation energy of carbon diffusion in ferrite	Qa	kJ/mol	10
Pre-exponential for diffusion of carbon	D_0	m2/s	80
Gas constant	R	J/mol.K	6.10-5
Steel carbon content	C		0.34 %
Austenite carbon content	Ce		0.8 %
Ferrite carbon content	Cf		0.01 %
Critical value of carbon content	Cc		0.05 %
Volume fraction of pearlite colonies	fi		0.5375

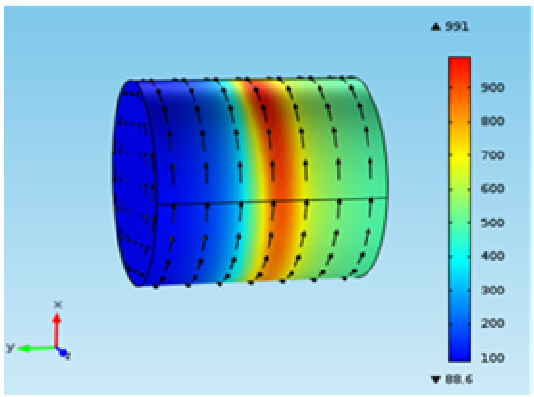

Fig. 4. Simulation results - Temperature distribution.

power directly affects the rate of heating and cooling and subsequently affects the microstructure obtained. The influence of rotational speed becomes negligible at and above 4000 rpm. With a rotational speed of 1000 rpm, a scanning speed of 5 mm/s and a power of 1550 W, the temperature reach 1800 °C (Fig. 7).

It is clear from Fig. 8 that an increase in scanning speed decreases treatment, both in terms of time and temperature. With a scanning speed of 2 mm/s, the temperature reached is greater than the melting temperature. The heating and cooling speed increase proportionally according to the scanning speed.

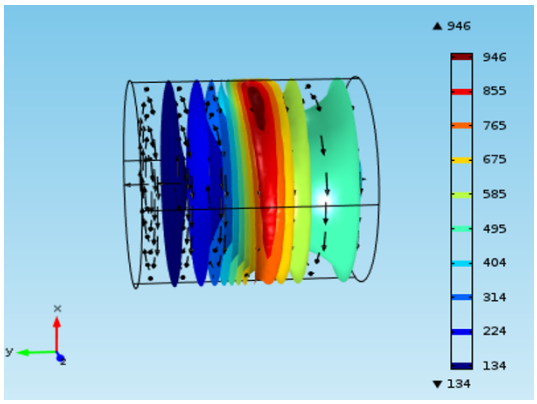

Fig. 5. Simulation results - Heat flux distribution.

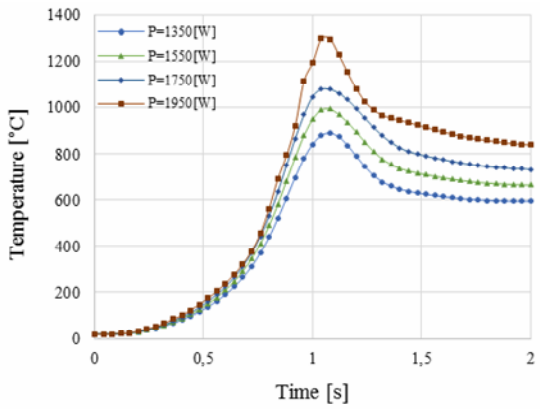

Fig. 6. Influence of laser power on temperature and heating time (W = 4000 [rpm] and V = 5 [m/s]).

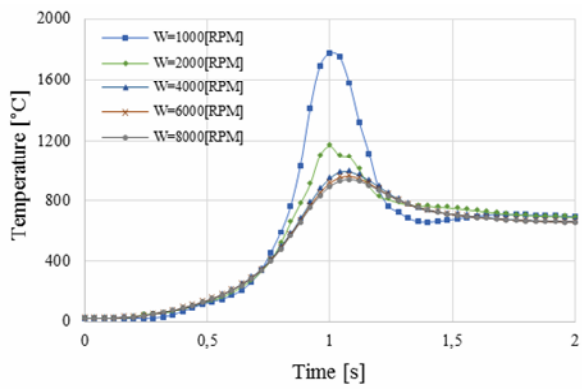

Fig. 7. The influence of rotational speed on the temperature and time of treatment (P = 1550 [W] and V = 5 [m/s]).

5. Experimental validation

The experiments were done with an AISI 4340 steel cylinder 10 mm in diameter. The specimen is mounted on a

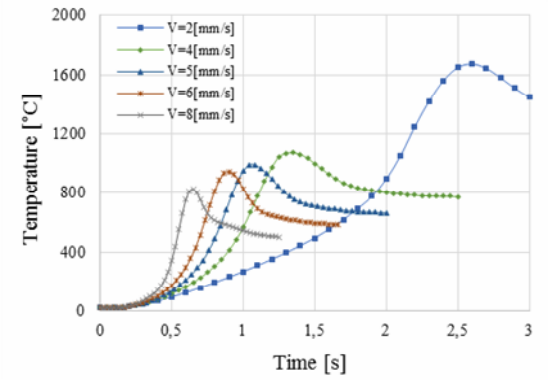

Fig. 8. Influence of rotational speed on temperature and heating time (P = 1550 [W] and V = 5 [m/s]).

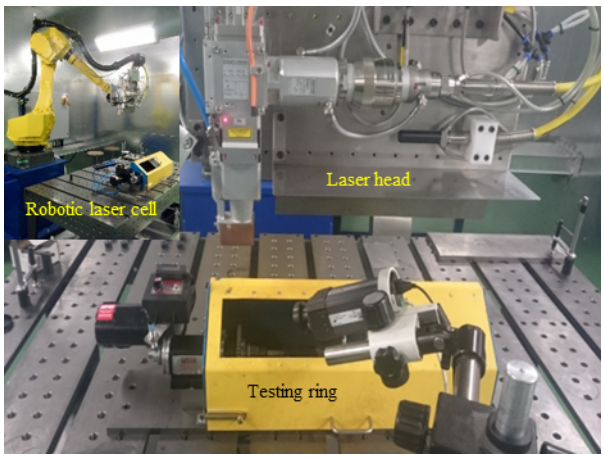

Fig. 9. Robotic heat treatment laser cell used for the experimentation.

test stand that could reach rotation speeds up to 10000 rpm. The laser used is Nd type: YAG. The laser head is mounted on a Fanuc robot with six degrees of freedom.

Fig. 9 shows the experimental setup. The specimens are treated by hardening and tempering to ensure a core hardness of 35 HRC. The micro hardness is measured using a Clemex device. Four experiments were conducted with a random choice of parameters to validate the finite element model. An algorithm based metallurgical formulations coupled with Matlab can process the simulation results on COMSOL.

Practical experiments are performed with a confidence interval of 95 % (Table 3). Figs. 10 and 11 show the relative deviations between the practical measures and the simulation results that are acceptable for 3D model validation. For tests 1 and 3, the relative error varies between 3.5 % and 11 %. The relative errors for tests 2 and 4 are under 1 %.

6. Statistical analysis

The objective of this part is to identify the influence of various parameters on the hardened depth. This is achieved using an experiment design, consisting in producing a series of N experiments and determining the value of the hardened depth

Table 3. Factors and levels for validation tests.

Test	P (W)	V (mm/s)	W (rpm)
1	1750	5	4000
2	1550	5	4000
3	1300	4	2000
4	1500	8	4000

Table 4. Factors and levels for ANOVA.

Factor	Symbol	Units
Power	P	W
Scanning speed	V	mm/s
Speed of rotation	W	rpm

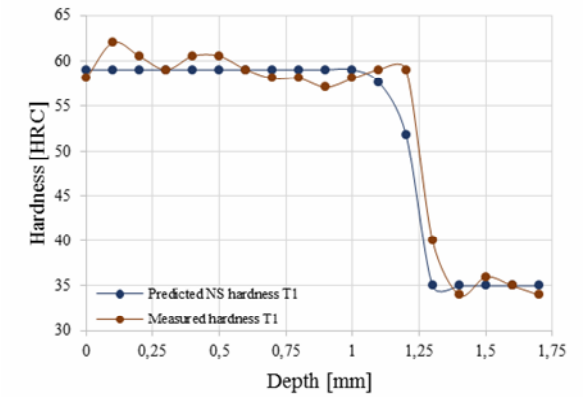

Fig. 10. Typical hardness curve – Case of test 1.

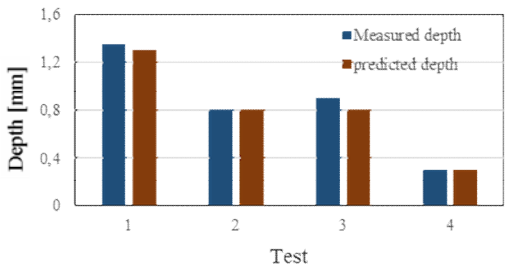

Fig. 11. Experimental validation of the hardened depth.

for various combinations. So, in this case, the selected solution is the hardened depth profile represented by the three characteristic $\{H_1, D_1, D_2\}$. The experiments are carried out using a 3D model with COMSOL software (see Figs. 4 and 5).

The factors to be examined in this study are power, rotary speed and scanning speed (Table 4). The Analysis of the variance (ANOVA) is a basic tool in determining the significance of a particular effect or a mathematical model. The principle of the analysis of variance is based on calculating the total difference between the results of modelled experiments and the average of those measurements.

ANOVA is a computational technique which is used to estimate the relative significance of each process parameter in terms of percent contribution to the overall response. The pa-

Table 5. Experimental planning (L_{27}).

Test	*P*	*V*	*W*
1	1300	4	2000
2	1300	4	4000
3	1300	4	6000
4	1300	6	2000
5	1300	6	4000
6	1300	6	6000
7	1300	8	2000
8	1300	8	4000
9	1300	8	6000
10	1500	4	2000
11	1500	4	4000
12	1500	4	6000
13	1500	6	2000
14	1500	6	4000
15	1500	6	6000
16	1500	8	2000
17	1500	8	4000
18	1500	8	6000
19	1700	4	2000
20	1700	4	4000
21	1700	4	6000
22	1700	6	2000
23	1700	6	4000
24	1700	6	6000
25	1700	8	2000
26	1700	8	4000
27	1700	8	6000

rameters with higher percent contributions are ranked higher in terms of importance in the experiment, and also have significant effects in controlling the overall response [12, 13]. Among several existing plans, the Taguchi orthogonal plan minimizes the effect of aliases and measures error with minimum testing. In this context, an orthogonal plan L_{27} of 3 factors to 3 levels was chosen (Table 5). The results of the tests presented Table 6 show that in this case the factors {*P*, *V*} and the interaction {*PV*} have a P-value less than 0.005, which means that there are 0.05 in 100 chances that the true value of the coefficient {*P*, *V*, *W*, *PV*} will be zero. This confirms the significance of the power, the scanning speed, the rotational speed, and the interaction between the power and the scanning speeds in the model.

The influence of the other terms is not significant in controlling the overall response [13]. The results of Fig. 12 confirm the preliminary simulation results, showing a remarkable influence of scanning speed and power. On the other hand, the influence of the rotation speed is negligible in relation to the other factors. The contribution of power to the hardened depth is 18.91 %, and the contribution of the scanning speed is about

Table 6. ANOVA for hardened depth (D_2).

Source	DF	Sum of squares	Mean square	F-Value	P-Value	C (%)
P	2	1.33725	0.5933	584.65	0.000	18.91
V	2	4.77970	0.2189	215.73	0.000	67.60
W	2	0.05899	0.0117	11.53	0.004	0.83
P.V	4	0.88339	0.2208	217.62	0.000	12.49
P.W	4	0.00170	0.0004	0.42	0.791	0.02
V.W	4	0.00166	0.0004	0.41	0.742	0.02
Error	8	0.00812	0.0010	-	-	0.11
Total	26	7.07081	-	-	-	100

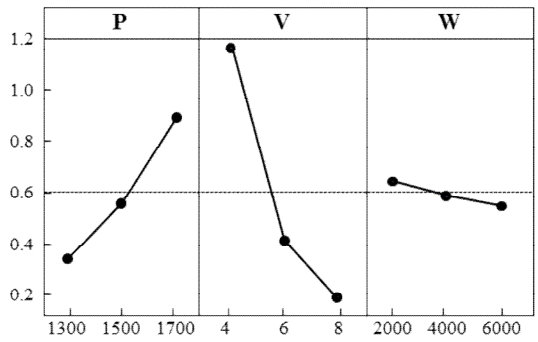

Fig. 12. Effect of various parameters on the hardened depth (D_2).

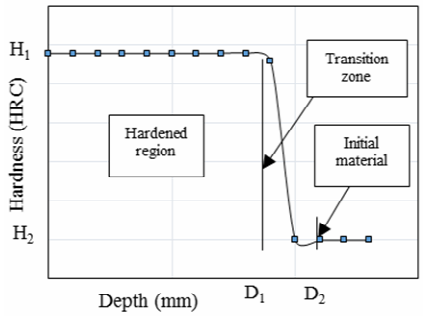

Fig. 13. Typical hardness curve.

67.60 %. The contribution rotation speed is low, on the order of 0.83 %. The interactions of power with the scanning speed have a combined contribution of about 12.49 %.

7. Artificial neural network prediction model

The objective of this section is to create a model of artificial neural networks capable of predicting the hardness and the hardened depth. The curve describing the hardness profile is divided into three zones. The first is the hardened zone, consisting of 100 % martensite. The second is the transition zone, consisting of ferrite, pearlite and martensite. The third zone is the untreated area. For this reason, we define the four points {H_1, H_2, D_1, D_2}: The first two sets are used to define the hardness and the others to define the depth (Fig. 13). The artificial neural network is a very powerful model in terms of its

Table 7. Experimental planning for training data.

Factor	Levels				
P	1200	1400	1600	1800	2000
V	4	5	6	7	8
W	1000	2000	3000	4000	5000

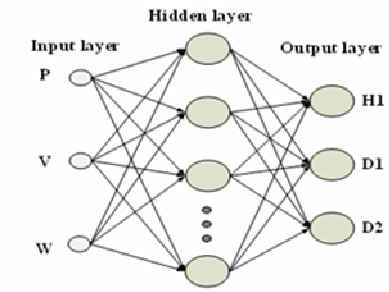

Fig. 14. The ANN based model structure.

precision in prediction, inspired by the biological neuron. A neuron is a tiny structure that treats nerve impulses that arrive (inputs), each according to its relative importance, and emits only one output signal (output).

Artificial neurons reproduce the same process, receiving each input signal (input) tempered by a weight (weight). These weights are also called synaptic weights by analogy. The weighted inputs, usually ordered, are then compared to an activation threshold and passed in the function of the neuron, which produces the output (output) desired [14, 15]. In this study, a Multilayer Perceptron neural network model with one hidden layer containing 10 neurons is chosen (see Fig. 14). The number of intermediate layers depends on the complexity of the problem to be dealt with. The inputs to the system are the scanning speed, the rotation speed and the laser power, but the outputs are the limits of the hardness curve: H_1, D_1, D_2.

The design used in the ANOVA study is chosen mainly to determine the interactions of different factors. In addition, it does not present a rich database for a neural network. For this another orthogonal design was chosen in order to have given a more complete database. The selected plan is the L_{25} Taguchi plan (Table 7). It consists of three factors on five levels. A neural network model of 3 inputs and 2 two outputs was established. The three input parameters are *P*, *V* and *W*. The output parameters are the hardened depths D_1 and D_2. A single hidden layer of 10 neurons was used. The sigmoid function is used as the activation function. Furthermore, the value of the coefficient of determination, R^2 = 99.58 %, is good, which indicates that the model is relatively well adjusted. Therefore, there is a good correlation between the measured values and the calculated ones (Fig. 15 and Table 8). Another neural network model of three inputs and one output was also established. The three input parameters are *P*, *V* and *W*. The output parameter is the hardness depth, H_1.

An orthogonal matrix L_9, based on the Taguchi method, was used in the validation experiments [12]. The validation

Table 8. Coefficients of determination for the ANN prediction model.

	Rtraining	Rvalidation	Rtest	Rtotal
Depth	0.99583	0.94104	0.95329	0.97701
Hardness	0.99313	0.95427	0.9732	0.97909

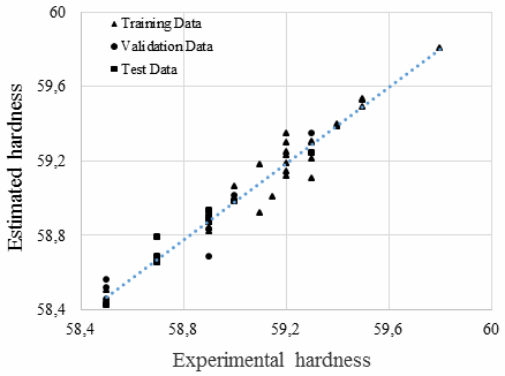

Fig. 15. Scatter plots of simulation and prediction of $\{D_1, D_2\}$.

matrix illustrated in Table 9 is injected into the same neural network programs previously used. The results found in the validation are satisfactory and show that the model is reliable in predicting the hardness based on other input parameter.

Table 8 shows that the values of the coefficients of determination of the validation tests of the points $\{D_1, D_2\}$ and $\{H_1\}$ are 94.104 and 95.427, respectively. This implies a very good capacity for prediction. Two practical tests were planned to validate the results of the neural networks (Figs. 16 and 17). With a power of 1500 W, a scanning speed of 4 mm/s, and a rotary speed of 4000 rpm, the relative errors is 11 % in prediction of the D_1 point, and 0 % in prediction of the D_2 point. As a conclusion the method of neural networks is very reliable in terms of prediction, and enables manufacturers to create a rich and an accurate database.

8. Conclusions

In this study, a comprehensive approach developed to design an effective prediction model for hardness profile of AISI 4340 steel heat treated by laser is presented. Several laser hardening parameters and conditions were analysed and their correlation with multiple performance characteristics of hardened surface was investigated using a structured experimental investigations and exhaustive 3D numerical simulations under consistent practical process conditions.

After identifying the hardening parameters and conditions that provide the best information about the laser heating and the surface hardening transformation processes, an ANN based modelling approach was proposed to build an accurate and consistent hardness profile prediction model. The resulting model demonstrates that the ANN modelling approach can be used to achieve an accurate predicting model. Globally, the performance of the hardness profile prediction model shows significant improvement as compared to conventional meth-

Table 9. Experimental planning for validation data.

Factor	Levels		
P	1300	1400	1600
V	4	5	6
W	3000	4000	5000

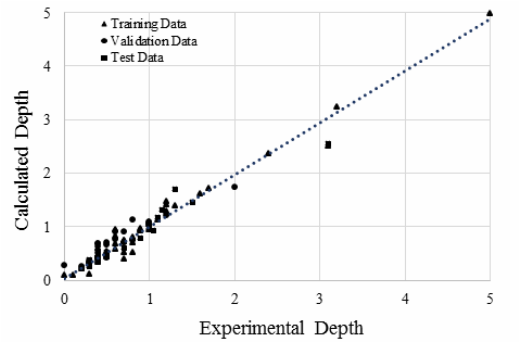

Fig. 16. Scatter plots of simulation and prediction of H_1.

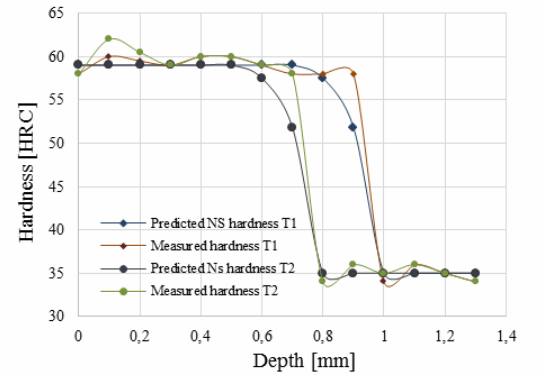

Fig. 17. Validation results for the ANN prediction model.

ods such as multiple regression analysis. With a global maximum relative error less than 11 % under various conditions, the prediction model can be considered efficient and have led to conclusive results, due to the complexity of the heat treatment process.

References

[1] S. Soundarapandian and R. Kovacevic, Hardness prediction in multi-pass direct diode laser heat treatment by on-line surface temperature monitoring, *Journal of Materials Processing Technology*, 212 (11) (2012) 2261-2271.

[2] R. Patwa and Y. C. Shin, Predictive modeling of laser hardening of AISI5150H steels, *International Journal of Machine Tools and Manufacture,* 47 (2) (2007) 307-320.

[3] J. C. Rozzi et al., Transient thermal response of a rotating cylindrical silicon nitride workpiece subjected to a translating laser heat source, part I: comparison of surface temperature measurements with theoretical results, *Journal of Heat transfer,* 120 (4) (1998) 899-906.

[4] J. C. Rozzi et al., Transient, three-dimensional heat transfer model for the laser assisted machining of silicon nitride: I. Comparison of predictions with measured surface temperature histories, *International Journal of Heat and Mass Transfer,* 43 (8) (2000) 1409-1424.

[5] S. Skvarenina and Y. C. Shin, Predictive modeling and experimental results for laser hardening of AISI 1536 steel with complex geometric features by a high power diode laser, *Surface and Coatings Technology*, 201 (6) (2006) 2256-2269.

[6] L. Orazi et al., Laser surface hardening of large cylindrical components utilizing ring spot geometry, *CIRP Annals - Manufacturing Technology*, 63 (1) (2014) 233-236.

[7] N. Barka and A. El Ouafi, Effects of laser hardening process parameters on case depth of 4340 steel cylindrical specimen - A statistical analysis, *Journal of Surface Engineered Materials and Advanced Technology*, 5 (3) (2015) 124.

[8] M. Ilyes, A. El Ouafi and N. Barka, Prediction of 4340 steel hardness profile heat-treated by laser using artificial neural networks and multi regression approaches, *International Journal of Engineering and Innovative Technology*, 4 (6) (2014) 14-22.

[9] M. F. Ashby and K. E. Easterling, The transformation hardening of steel surfaces by laser beams - I. Hypo-eutectoid steels, *Acta Metallurgica,* 32 (11) (1984) 1935-1948.

[10] P. Maynier, J. Dollet and P. Bastien, *Prediction of microstructure via empirical formulae based on CCT diagrams, Hardenability Concepts With Applications to Steel*, Metallurgical Society of AIME (1978) 163-178.

[11] P. Maynier, B. Jungmann and J. Dollet, *Creusot-Loire system for the prediction of the mechanical properties of low alloy steel products, Hardenability concepts with Applications to Steel*, Metallurgical Society of AIME (1978) 518-545.

[12] R. L. Mason, R. F. Gunst and J. L. Hess, *Statistical design and analysis of experiments: with applications to engineering and science*, John Wiley & Sons (2003).

[13] B. Acherjee et al., Prediction of weld strength and seam width for laser transmission welding of thermoplastic using response surface methodology, *Optics & Laser Technology*, 41 (8) (2009) 956-967.

[14] S. K. Dhara, A. S. Kuar and S. Mitra, An artificial neural network approach on parametric optimization of laser micromachining of die-steel, *International Journal of Advanced Manufacturing Technology*, 39 (1) (2008) 39-46.

[15] G. Buffa, L. Fratini and F. Micari, Mechanical and microstructural properties prediction by artificial neural networks in FSW processes of dual phase titanium alloys, *Journal of Manufacturing Processes*, 14 (3) (2012) 289-296.

Mahdi Hadhri is a researcher student in the Department of Mathematics, Computer Science and Engineering at the University of Quebec at Rimouski. His research fields include manufacturing materials, manufacturing processes improvement, and quality management for industrial applications.

Abderrazak El Ouafi is a Professor in the Department of Mathematics, Computer Science and Engineering at the University of Quebec at Rimouski. He is also Director of Production and Automation Research Laboratory. His research interests are mainly oriented in precision engineering, manufacturing system design and control, improvement of manufacturing processes performance and intelligent control related to sensor fusion, neural networks and fuzzy control.

Noureddine Barka is an Assistant Professor in the Department of Mathematics, Computer Science and Engineering at the University of Quebec at Rimouski. His research fields include manufacturing materials, CAD/CAM, manufacturing processes improvement, and quality control for industrial applications.